The Astrophysical Journal, 882:167 (11pp), 2019 September 10 https://doi.org/10.3847/1538-4357/ab3b03

The Roles of Mass and Environment in the Quenching of Galaxies

E. Contini[1], Q. Gu[1], X. Kang[2], J. Rhee[3], and S. K. Yi[3]
[1] School of Astronomy and Space Science, Nanjing University, Nanjing 210093, People's Republic of China; emanuele.contini82@gmail.com
[2] Purple Mountain Observatory, the Partner Group of MPI für Astronomie, 2 West Beijing Road, Nanjing 210008, People's Republic of China
[3] Department of Astronomy and Yonsei University Observatory, Yonsei University, Yonsei-ro 50, Seoul 03722, Republic Of Korea
Received 2019 May 24; revised 2019 August 6; accepted 2019 August 12; published 2019 September 16

Abstract

We study the roles of stellar mass and environment in quenching the star formation activity of a large set of simulated galaxies by taking advantage of an analytic model coupled to the merger tree extracted from an *N*-body simulation. The analytic model has been set to match the evolution of the global stellar mass function since redshift $z \sim 2.3$ and give reasonable predictions of the star formation history of galaxies at the same time. We find that stellar mass and environment play different roles: the star formation rate/specific star formation rate–M_* relations are independent of the environment (defined as the halo mass) at any redshift probed, $0 < z < 1.5$, for both star-forming and quiescent galaxies, while the star formation rate–$M_{\rm halo}$ relation strongly depends on stellar mass in the same redshift range, for both star-forming and quiescent galaxies. Moreover, the star formation rate and the specific star formation rate are strongly dependent on stellar mass even when the distance from the cluster core is used as a proxy for the environment, rather than the halo mass. We then conclude that stellar mass is the main driver of galaxy quenching at any redshift probed in this study, not just at $z > 1$ as generally claimed, while the environment has a minimal role. All the physical processes linked to the environment must act on very short timescales, such that they do not influence the star formation of active galaxies, but increase the probability of a given galaxy to become quiescent.

Key words: galaxies: evolution – galaxies: general

1. Introduction

Galaxies are an important component of the visible matter in the universe. Given the diversity of their morphologies and general properties, they evolve as a consequence of several physical processes responsible for the different populations that we can observe in the local universe. A deep understanding of these processes, in particular the role of quenching and the time/mass scales involved, would end up in a significant step forward in the comprehension of galaxy formation and evolution.

It is well known that, broadly speaking, galaxies can be classified into two main populations according to their rate of star formation activity: star-forming systems and quiescent (passive) objects (Blanton et al. 2003; Baldry et al. 2004; Balogh et al. 2004; Brinchmann et al. 2004; Kauffmann et al. 2004; Cassata et al. 2008; Pallero et al. 2019; Davies et al. 2019). Star-forming galaxies actively form new stars, have blue colors and late-type morphologies, and are typically young (Blanton et al. 2003; Kauffmann et al. 2003; Noeske et al. 2007; Wuyts et al. 2011). On the other hand, quiescent galaxies do not show star formation activity, have red colors and early-type morphologies, and are typically old (Baldry et al. 2004; Gallazzi et al. 2008; Wetzel et al. 2012; van der Wel et al. 2014).

Galaxy properties are also found to be dependent on both environment and stellar mass. Generally speaking, galaxies in denser environments typically have early-type morphologies and are less star-forming, redder, older, and more metal-rich (Dressler 1980; Kauffmann et al. 2004; Cooper et al. 2010; Peng et al. 2010; von der Linden et al. 2010), and the same trends are still valid for more massive galaxies (Kauffmann et al. 2003; Baldry et al. 2006; Weinmann et al. 2006; Bamford et al. 2009; Peng et al. 2010). Environment and stellar mass have been found to be important for the quenching of galaxies, although we do not have a clear knowledge yet of which between environment and mass plays the most important role in galaxy quenching (it is sometimes referred to as the nature/nurture debate).

During the past years, many physical processes related to both environment and stellar mass have been invoked in order to explain galaxy quenching (Noeske et al. 2007; Peng et al. 2010; Sobral et al. 2011; Muzzin et al. 2012, 2013; Darvish et al. 2016; Trussler et al. 2018). In their pioneering work, Peng et al. (2010), who used SDSS and zCOSMOS data, demonstrated the mutual independence of stellar mass and environment in quenching star formation. From the empirical model they constructed, they were able to separate the effects of mass and environmental quenching, and found that mass quenching is the main process responsible for quenching star formation in galaxies with $\log M_* > 10.6$, independently of environment and redshift. On the other hand, environmental processes become important at low redshift and for low-mass galaxies. In short, massive galaxies are more likely quenched by internal processes that are independent of the environment in which they reside, and galaxies in denser environment are likely quenched by processes that are independent of their stellar mass.

Mass quenching generally refers to internal processes that mainly depend on the galaxy mass. Different processes have been proposed depending on the characteristic stellar mass regime. In the low-mass regime ($\log M_* < 9$), gas outflows driven by stellar feedback such as stellar winds/radiation or supernova explosions are thought to play an important part in quenching star formation (Larson 1974; Dekel & Silk 1986; Dalla Vecchia & Schaye 2008). For more massive galaxies ($\log M_* > 10$), in particular those with a pronounced bulge component, AGN feedback appears to be more effective in stopping star formation. The AGN can be powerful enough to

either heat up the surrounding cold gas by injecting energy via radio jets or winds, or even sweep away the gas content through powerful outflows (Croton et al. 2006; Fabian 2012; Fang et al. 2013; Cicone et al. 2014; Bremer et al. 2018).

Environmental quenching is usually intended as the process, or series of processes, that quench star formation because of interactions between galaxies and their surroundings, such as ram pressure stripping (Gunn & Gott 1972; Poggianti et al. 2017), strangulation or starvation (Larson et al. 1980; Moore et al. 1999), and harassment (Farouki & Shapiro 1981; Moore et al. 1996). Ram pressure stripping in clusters removes the cold gas in the interstellar medium (ISM) due to the interaction between it and the intracluster medium, thus inhibiting further star formation unless hot gas can cool and replenish the cold gas reservoir. Starvation (or strangulation) is a process that is assumed to be instantaneous as soon as a galaxy is accreted in a large system and that completely removes the hot gas available for cooling, thus shutting down the fuel for further star formation. Harassments are instead the result of close galaxy–galaxy encounters, which can lead to the removal of gas and the conversion of part of the cold gas into stars.

All of the above-mentioned mass/environmental processes can be otherwise classified as processes that act on central galaxies (mass quenching) and on satellite galaxies (environmental quenching). Centrals are either field galaxies or the most massive galaxies residing in the center of groups/clusters, while satellites were formerly centrals and became satellites once accreted into a larger system. This central/satellite dichotomy has often been used (especially on the theoretical side) as a parallelism with mass/environmental quenching (e.g., van den Bosch et al. 2008; Peng et al. 2012; Wetzel et al. 2013; Contini et al. 2017b).

In order to understand what quenching dominates during the evolutionary history of galaxies, it is necessary to separate their contributions. In the past few years, many studies focused on this point (e.g., Kauffmann et al. 2003; Muzzin et al. 2012; Koyama et al. 2013; Darvish et al. 2016; Laganá & Ulmer 2018 and references therein) to understand how the star formation rate (SFR) or colors depend on the halo mass/clustercentric distance at fixed stellar mass, which quantifies mass quenching, and how the SFR–M_* relations vary as a function of environment, which quantifies environmental quenching, at different redshifts. Although we know that stellar mass does play a role, the picture is not yet clear for what concerns the environment. A bunch of studies have found that galaxies are more likely to be quenched or red in more massive halos (see e.g., Balogh et al. 2000; De Propris et al. 2004; Weinmann et al. 2006; Blanton & Berlind 2007; Kimm et al. 2009), but others (e.g., Pasquali et al. 2009; Vulcani et al. 2010; Muzzin et al. 2012; Koyama et al. 2013; Darvish et al. 2016; Laganá & Ulmer 2018) have found no or little dependence on either halo mass or clustercentric distance.

In this paper, we make use of the analytic model described in Contini et al. (2017a, 2017b) coupled with a merger tree constructed from a high-resolution N-body simulation. The model has been developed in order to match the stellar mass function at high redshift and predict its evolution with time, with an average (1σ) precision of <0.1 dex in over three orders of magnitudes in stellar mass at $z \sim 0.3$. Our model treats the quenching of star formation according to an exponential decay of the star formation rate with time, which depends on several galaxy properties such as stellar mass or type (satellite/central). Environment and mass quenching are hence already implemented in our model. The primary goal of this paper is to identify the main quenching mode (mass or environment) as a function of redshift and compare our results with those available in the literature.

This paper is structured as follow. In Section 2, we describe the main features of our model and simulation. In Section 3, we present our results, which will be fully discussed in Section 4. In Section 5, we summarize the main conclusions of our analysis. Throughout this paper, we use a standard cosmology, namely $\Omega_\lambda = 0.73$, $\Omega_m = 0.27$, $\Omega_b = 0.044$, $h = 0.7$, and $\sigma_8 = 0.81$. Stellar masses are computed by assuming a Chabrier (2003) initial mass function (IMF).

2. Methods

In the following analysis, we use the prediction of an analytic model developed in Contini et al. (2017a) and refined in Contini et al. (2017b). We refer the readers to those papers for the details of the physics implemented, and we briefly describe here the main features. The model was run on the merger tree of an N-body simulation, the characteristics of which are fully mentioned in Kang et al. (2012) and briefly summarized in Contini et al. (2017a).

The analytic model uses the so-called subhalo abundance matching (ShAM) technique to populate dark matter halos with galaxies (e.g., Vale & Ostriker 2004), and its main goal is to predict the evolution of the global galaxy stellar mass function (SMF). For this purpose, the model is forced to match the observed SMF at $z_{\rm match} = 2.3$, such that the predicted and observed SMFs are the same. By reading the merger tree of the N-body simulation, the model sorts dark matter halos and at each time assigns a galaxy to each halo according to the stellar mass–halo mass relation valid at that particular redshift. Once galaxies are set, they evolve according to their merger histories, which are given by the merger tree, and to their star formation histories (SFHs). The evolution of the SFR is the novelty in our model. At $z_{\rm match}$ (or the redshift when they are born if $z_{\rm form} < z_{\rm match}$), an SFR is assigned to each galaxy by means of the SFR–M_* relation observed at that redshift, and the SFR will evolve down to the present time (unless the galaxy merges or is disrupted) according to the τ model described in Contini et al. (2017b), depending on the galaxy type (central or satellite). Moreover, due to gravitational interactions with their host halos, galaxies might lose a given amount of stellar mass once they are accreted into a larger system (i.e., they become satellites). The model does consider stellar stripping,[4] and the details of the implementation can be found in Contini et al. (2017a).

2.1. Mass and Environmental Quenching Prescriptions

For the purposes of this paper, it is worth to fully describe the decay with time of the SFR (τ model) for both central and satellite galaxies, as it basically accounts for the mass and environmental quenching. As explained above, the model first assigns an SFR to each galaxy according to the SFR$-M_*$ relation either at $z = z_{\rm match}$ or at $z = z_{\rm form}$, in case a galaxy forms after $z_{\rm match}$. From that redshift on, the SFR evolves according to functional forms that consider information such as

[4] Stellar stripping has been proven to be the main channel for the formation of the intracluster light in galaxy groups and clusters. For further details on this topic, see Contini et al. (2014, 2018, 2019) and references therein.

type (central or satellite), stellar mass, and a quenching timescale. The SFHs of centrals and satellites are treated separately. For centrals, we use a prescription very similar to the one adopted in Noeske et al. (2007):

$$\mathrm{SFR}_{\mathrm{cen}}(t) = \mathrm{SFR}_{\mathrm{match/form}} \cdot \exp\left(-\frac{t}{\tau_c}\right), \quad (1)$$

where τ_c is the quenching timescale of centrals. τ_c is derived from the following equation:

$$\tau_c = 10^{11.7} \cdot \left(\frac{M_*}{M_\odot}\right)^{-1} \cdot (1+z)^{-1.5}\ [\mathrm{Gyr}], \quad (2)$$

where M_* is the stellar mass at $z = z_{\mathrm{match/form}}$, $\pm 20\%$ random scatter assigned as a perturbation. Our prescription differs from the original one (Noeske et al. 2007) as we consider only the stellar mass (rather than the baryonic mass) and add a redshift-dependent correction.

The SFHs of satellites are modeled in a similar manner. Our approach is a revised version of the so-called delayed-then-rapid quenching mode suggested by Wetzel et al. (2013), where the SFRs of satellites evolve like those of centrals for 2–4 Gyr after infall, and then quench rapidly according to a quenching timescale τ_s. We distinguish between two kinds of satellite galaxies: satellites that were accreted before z_{match}, and those accreted after it. In the first case, the quenching timescale τ_s is assigned at z_{match} by Equation (2), and we assume no delayed quenching. In the second case, the quenching timescale τ_s is assigned at the redshift of accretion z_{accr} and is assumed to be a random fraction f_τ between 0.1 and 0.5 of τ_c. Hence, the SFR of satellites evolves as described by Equation (1) if

$$t_{\mathrm{since\ infall}} < t_{\mathrm{delay}},$$

where t_{delay} is randomly chosen in the range 2–4 Gyr, and as

$$\mathrm{SFR}_{\mathrm{sat}}(t) = \mathrm{SFR}_{\mathrm{match/form}} \cdot \exp\left(-\frac{t}{\tau_s}\right) \quad (3)$$

thereafter. $\mathrm{SFR}_{\mathrm{match/form}}$ in Equations (1) and (3) is set at $z = z_{\mathrm{match/form}}$ and derived by following Equation (2) in Tomczak et al. (2016):

$$\log(\mathrm{SFR}\ [M_\odot\ \mathrm{yr}^{-1}]) = s_0 - \log\left[1 + \left(\frac{M_*}{M_0}\right)^{\gamma}\right], \quad (4)$$

where s_0 and M_0 are in units of $\log(M_\odot\ \mathrm{yr}^{-1})$ and $M_\odot$, respectively. As a perturbation, the model adds a random scatter in the range ± 0.2 dex. s_0 and M_0 are given by (Equation (3) in Tomczak et al. 2016)

$$\begin{aligned} s_0 &= 0.195 + 1.157z - 0.143z^2 \\ \log(M_0) &= 9.244 + 0.753z - 0.090z^2 \\ \gamma &= -1.118. \end{aligned} \quad (5)$$

Equation (4) and the set of Equations (5) altogether define the evolution with time of the SFR–M_* relation with a mass-dependent slope (for more details about the necessity of a mass-dependent slope, see, e.g., Leja et al. 2015; Tomczak et al. 2016; Contini et al. 2017a, 2017b). A schematic representation of how the quenching model works is shown in Figure 1.

This model considers both environmental and mass quenching. The environmental quenching is explicitly included in Equations (1) and (3), and it is much faster for satellite galaxies. The mass quenching (different from the one described in Peng et al. 2010) is implemented in the calculation of the quenching timescales, such that, for both satellite and central galaxies, the quenching is faster with increasing stellar mass and redshift.

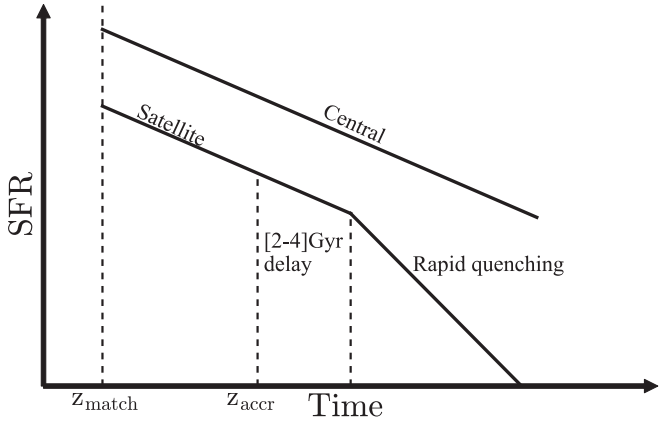

Figure 1. Schematic representation of our quenching model for both centrals and satellites. The SFR of central galaxies is set at $z = z_{\mathrm{match/form}}$ and then decays as shown in Equation (1). The SFR of satellite galaxies decays similarly to that of centrals for a "delayed" period after accretion, followed by a rapid quenching (given by τ_{sat}) right after.

3. Results

In this section, we present our analysis and highlight the main results, which will be fully discussed in Section 4 and compared with recent studies on the same topic. All units are h corrected, such that masses are expressed in $M_\odot$, SFR in $M_\odot$/yr, specific star formation rate (SSFR;which is defined as SFR/M_*) in yr^{-1}, and densities in $M_\odot/\mathrm{Mpc}^3$.

For the purposes of our analysis, we need to split the sample of galaxies into star-forming and quiescent. The separation is quite arbitrary: color separation (e.g., Muzzin et al. 2012; Koyama et al. 2013), by using an offset from the star-forming sequence (e.g., Trussler et al. 2018; Davies et al. 2019), or an SSFR cut (e.g., Wetzel et al. 2012; Laganá & Ulmer 2018; De Lucia et al. 2019). We use a redshift-dependent SSFR cut and select as star-forming all galaxies with SSFR higher than t_{hubble}^{-1}, which translates in $\sim 10^{-10}\ \mathrm{yr}^{-1}$ at $z = 0$ (Franx et al. 2008; De Lucia et al. 2019).

Figure 2 shows the fraction of quiescent galaxies as a function of stellar mass as predicted by our model (solid lines), and observed data (black stars and 3σ error bars) by Wetzel et al. (2012) extracted from the SDSS Data Release 7 (Abazajian et al. 2009), for galaxies in groups/clusters of different mass as shown in the legends, at $z \sim 0.1$. For this plot only, in order to make a fair comparison with observed data, we use the same SSFR cut used by Wetzel et al. (2012), i.e., $\mathrm{SSFR} = 10^{-11}\ \mathrm{yr}^{-1}$. Our model predictions agree fairly well with the observed data in a wide range of halo mass, from small groups ($\log M_{\mathrm{halo}} \sim 13$) to clusters ($\log M_{\mathrm{halo}} \sim 15$).

To check whether the model is also able to predict the distribution of stellar mass as a function of redshift, as it is supposed to, as it has been set to describe the evolution of the stellar mass function, in the left panel of Figure 3, we plot the stellar mass density as a function of redshift (red solid line), compared with observed data by Muzzin et al. (2013) from the COSMOS/UltraVISTA survey. As expected, the model

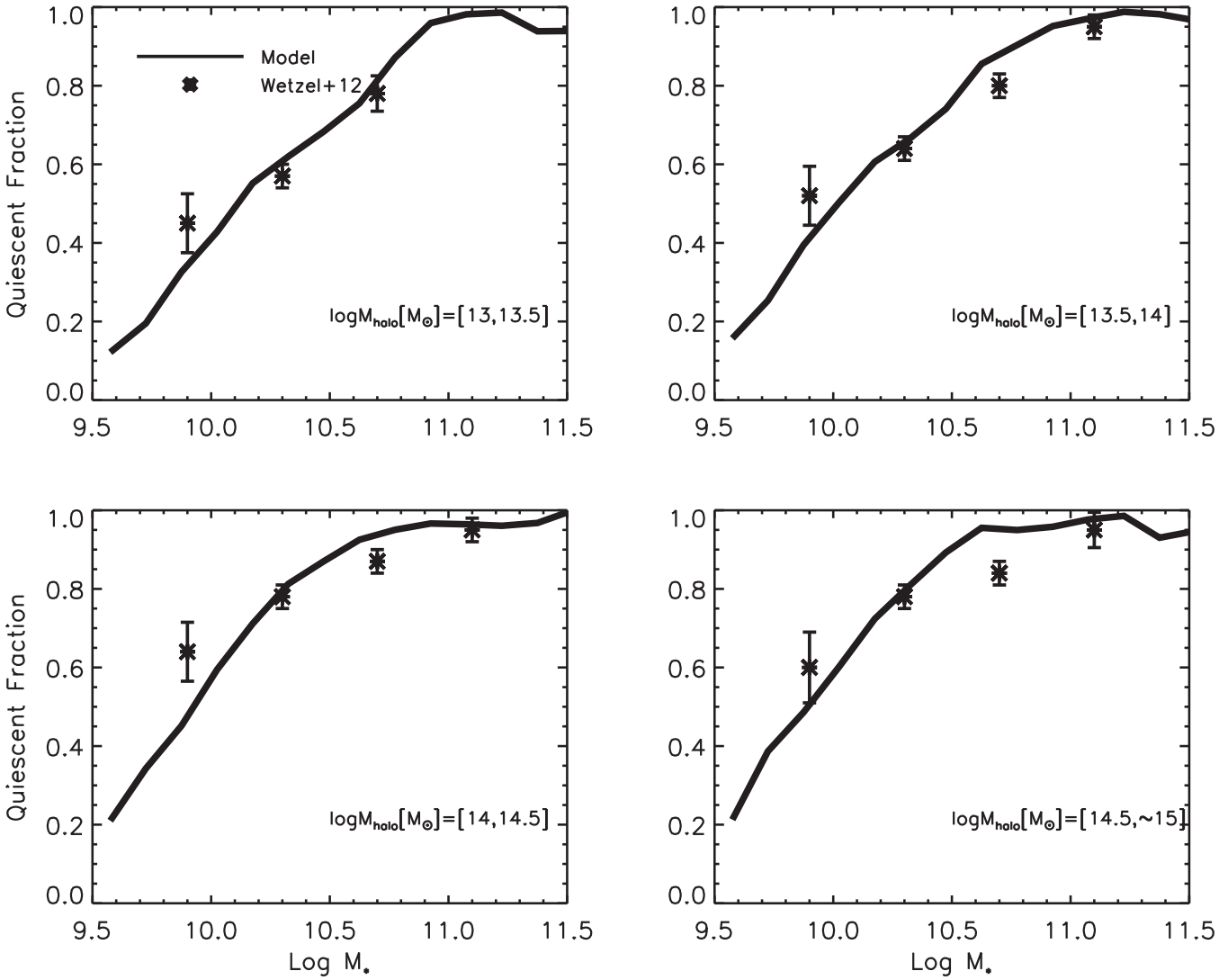

Figure 2. Fraction of quiescent galaxies (black lines) as a function of stellar mass in different halo mass bins (different panels) at $z \sim 0.1$ compared with observed data (black crosses) by Wetzel et al. (2012).

matches the observation within 2σ at high redshift, and within 1σ at $z < 1$. If we plot the same quantity (right panel of Figure 3) for star-forming (blue line and circles) and quiescent (red line and circles) galaxies, we find a mismatch between our model and observed data such that the model underpredicts the stellar mass density of quiescent galaxies and so overpredicts that of star-forming galaxies, independently of redshift. This is a consequence of the fact that the model is not able, according to our definition of quiescent galaxies, to predict their fraction as a function of redshift when compared with Muzzin et al. (2013) data. It must be noted that a large part of the tension can be due to the different criteria for separating the quiescent samples: a color separation in Muzzin et al. (2013) and a redshift-dependent SSFR cut in this work. This is not going to invalidate the rest of the analysis. Indeed, as pointed out by Wetzel et al. (2012), color cuts can overestimate the fraction of quiescent galaxies because of dust reddening (see also Maller et al. 2009). In the worst case scenario, it might be that our model overestimates the SFR history of low-mass galaxies (as shown by Figure 2), and this would in principle affect the environmental quenching efficiency in that stellar mass range, because low-mass galaxies are generally believed to be quenched by the environment (e.g., Weisz et al. 2015; Fillingham et al. 2016). However, even if our analysis is biased for this potential problem, we believe that the results we are going to show are robust in terms of the dependence on the environment, because the quiescent fractions of low-mass galaxies are low at any halo mass investigated. This potential issue is going to be a key point in a forthcoming paper currently in preparation.

Keeping in mind this caveat, we proceed in our analysis by going directly to the main points of the paper, i.e., the roles of mass and environment in quenching galaxies.

3.1. Environmental Quenching

It has been pointed out by several authors (e.g., Muzzin et al. 2012; Wetzel et al. 2012; Koyama et al. 2013; Darvish et al. 2016; Laganá & Ulmer 2018) that in order to extract the dependence of the SFR (and so SSFR) on stellar mass/environment, one has to study the quantity at fixed environment/stellar mass. In Figure 4, we focus on the role of the environment in shaping the SFR of galaxies by plotting the SFR–M_* relation for galaxies residing in clusters of different masses (different colors), for star-forming (solid lines) and

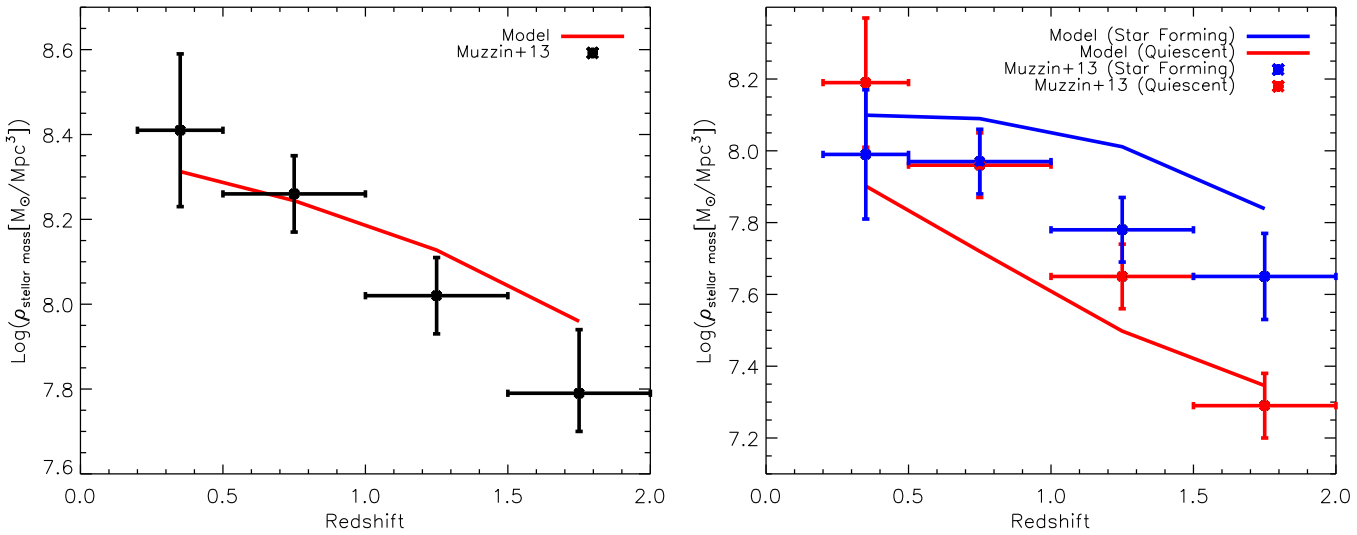

Figure 3. Left panel: evolution of the stellar mass density for the entire population of galaxies (red line) as a function of redshift, compared with observed data (black crosses) by Muzzin et al. (2013). Right panel: same as the left panel but for star-forming (blue line and blue crosses) and quiescent (red line and red crosses) galaxies.

quiescent (dashed lines) galaxies at different redshifts (different panels). As clearly shown by the plots, the environment (defined here as the halo mass in which galaxies reside) does not play any role in the SFR–M_* relation for both star-forming and quiescent galaxies, at any redshift investigated. This result is in perfect agreement with other studies, e.g., with Koyama et al. (2013), who studied the environmental dependence of the SFR–M_* relation for star-forming galaxies since $z \sim 2$ with H_α emitters in clusters and field environments. They conclude that such relation for star-forming galaxies is independent of the environment at any epoch, even considering dust attenuation. We support their results and extend the same conclusion to quiescent galaxies, although some environmental dependence is seen for very massive quiescent galaxies.

Figure 5 shows the same information shown by Figure 4, but for the SSFR. As for the SFR, the SSFR at fixed stellar mass is independent of environment, for both star-forming and quiescent galaxies (although again, the very massive quiescent galaxies seem to show some dependence). Our results agree well with previous studies (e.g., Muzzin et al. 2012; Laganá & Ulmer 2018). Muzzin et al. (2012) studied the effects of stellar mass and environment on the SFR and SSFR of galaxies in the redshift range $0.8 < z < 1.2$ for a spectroscopically selected sample of galaxies in clusters and field extracted from the Gemini Cluster Astrophysics Spectroscopic Survey. They find that, once the SSFR is plotted at a fixed stellar mass, it is independent of the environment. It is worth noting that, however, their definition of environment is the clustercentric distance, rather than halo mass. Moreover, for the least massive ($\log M_* \lesssim 9.3$) star-forming galaxies, there seems to be a trend with decreasing redshift for which both the SFR and SSFR decrease with increasing halo mass, which might be a hint of environmental dependence at least in that stellar mass range. However, we note that the average difference in that stellar mass range between the two extreme halo mass bins is less than 0.2 dex, i.e., within the typical SFR dispersion around the main sequence of star-forming galaxies.

3.2. Mass Quenching

We now move the subject of the analysis to the role of mass quenching, i.e., we study the SFR and SSFR as a function of environment (defined as halo mass) at fixed stellar mass. Figure 6 shows the SFR of star-forming (solid lines) and quiescent (dashed lines) galaxies as a function of halo mass, for galaxies in different stellar mass bins as indicated in the legend, and at different redshifts (different panels). The SFR is independent of halo mass (as found above) at any redshift, and the interesting feature is that, at a given halo mass, the SFR is strongly dependent on stellar mass, for both star-forming and quiescent galaxies. Indeed, in a range of three orders of magnitude in halo mass, the average difference between the SFR of the least massive stellar mass range ($8.5 < \log M_* < 9.25$) and the SFR of the most massive one ($10.75 < \log M_*$) at $z = 0$ is $\sim$1.6 dex for star-forming galaxies, and slightly higher for quiescent galaxies.

A similar trend in Figure 7 is found for the SSFR of the star-forming sample, while the trend does not appear clearly for the quiescent one. However, it must be noted that the average gap in SSFR for star-forming galaxies at $z = 0$ is $\sim$0.5 dex. Moreover, less massive galaxies are those more star-forming among all galaxies, in good agreement with previous studies (e.g., Peng et al. 2010), and in general with the downsizing scenario for which less massive galaxies quench on longer timescales (e.g., Popesso et al. 2011; Sobral et al. 2011; Fossati et al. 2017; J. Rhee et al. 2019, in preparation; Pintos-Castro et al. 2019).

We now want to see whether stellar mass quenching is dependent on the definition of the environment and so, instead of using the halo mass as a proxy of the environment, we plot the same quantities as a function of clustercentric distance. This is done in Figure 8, which shows the SFR (left panel) and SSFR (right panel) of star-forming (solid lines) and quiescent (dashed lines) galaxies as a function of distance from the halo center, for galaxies in different stellar mass bins, at $z = 0$. With respect to Figure 6, where the environment was defined as the mass of the cluster in which galaxies reside, the general trends and average gaps between the two extreme ranges in stellar mass do not change much (exception made for the SSFR of quiescent galaxies). The results found in Figures 6 and 8 strongly suggest that at fixed environmental conditions, maybe those given by the typical halo mass or clustercentric distance, the SFR and SSFR depend on stellar mass. The predictions of

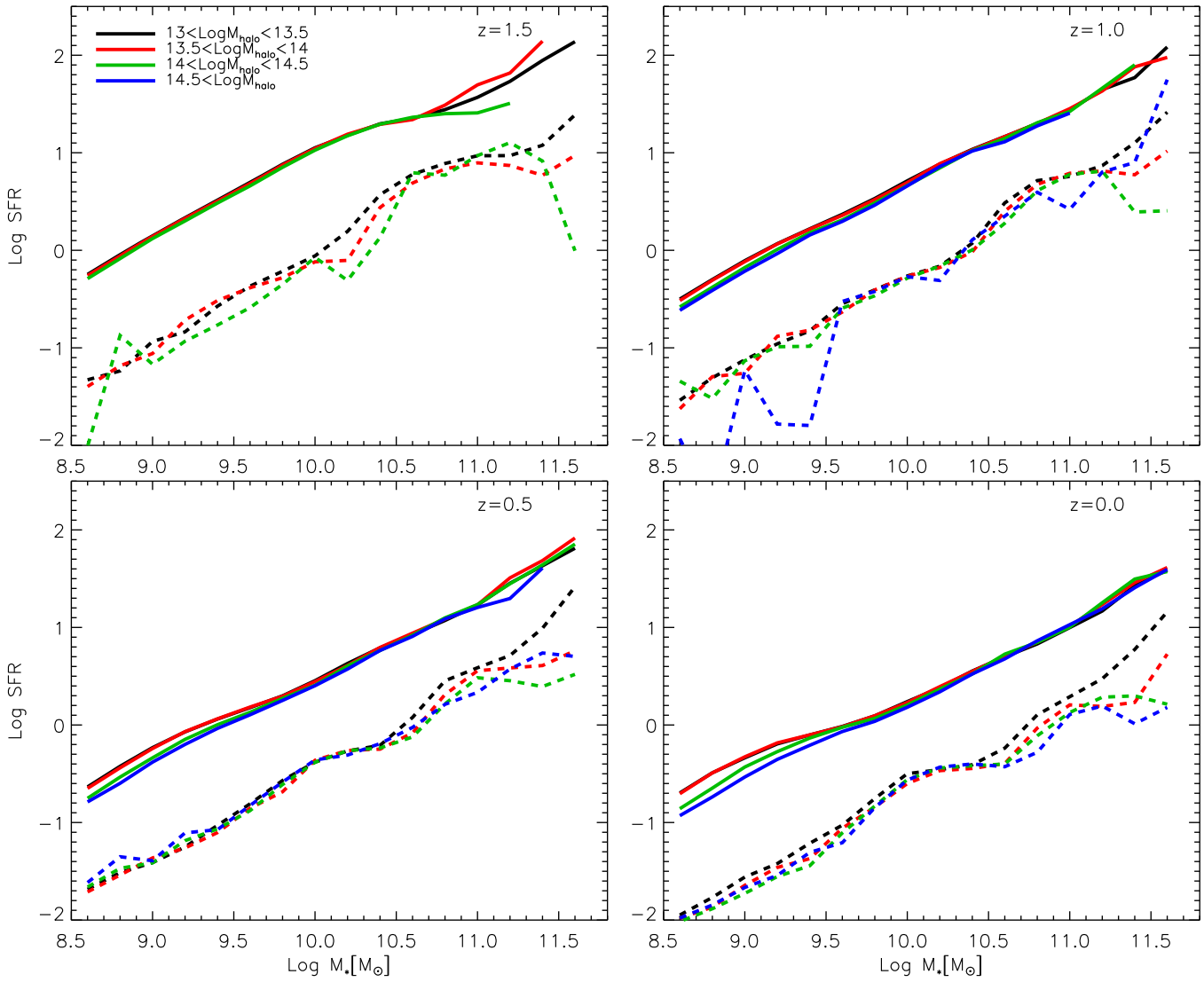

Figure 4. Evolution of the star formation rate–stellar mass relation as a function of redshift (different panels) for star-forming (solid lines) and quiescent (dashed lines) galaxies residing in halos of different mass, as indicated in the legend. The average 1σ scatter is around 0.2/0.25 dex for star-forming/quiescent galaxies, mostly independent of redshift and halo mass. Clearly, the environment does not play any role in the SFR–M_* relation for both star-forming and quiescent galaxies, at any redshift investigated.

our model agree well with many observational results in the literature (e.g., Muzzin et al. 2012; Koyama et al. 2013; Laganá & Ulmer 2018). We will compare our results with previous findings and fully discuss their implications in Section 4.

4. Discussion

The main goal of this work is to study the roles of mass and environmental quenching separately. Our analytic model was developed with the purpose of describing the evolution of the galaxy stellar mass function from high to low redshift and, at the same time, to give a reasonable prediction of the evolution of the SFR–M_* relation which agrees with that of the SMF. The model follows the SFH of each galaxy and treats them differently depending on their type (central or satellite) and on their quenching timescale (which is mass and redshift dependent). Hence, the effects of environment and mass are robustly considered. Simply put, central galaxies actively form stars for a given time that depends on their quenching timescale, but when they become satellites, they keep forming stars as they are active centrals for a few gigayear and experience rapid quenching later on. Such a model predicts different roles for mass and environment in quenching galaxies, which are important at different redshifts, and in a nonlinear relation with the galaxy stellar mass. Below we discuss them and their implications according to the results obtained in the analysis done in Sections 3.1 and 3.2.

In Figures 4 and 5, we analyzed the dependence on time of the SFR–M_* (Figure 4) and SSFR–M_* (Figure 5) relations for galaxies in different environments defined as the halo mass, from $z = 1.5$ to $z = 0$. Our results are consistent with a scenario where the environmental processes play a marginal role in galaxy quenching, at any time, or they are very rapid in such a way that the net environmental quenching is not seen. This scenario is supported by a number of observational achievements (e.g., Peng et al. 2010; Sobral et al. 2011; Muzzin et al. 2012; Koyama et al. 2013; Laganá & Ulmer 2018).

Very recently, Laganá & Ulmer (2018), who analyzed the relation between the SFR and SSFR as a function of

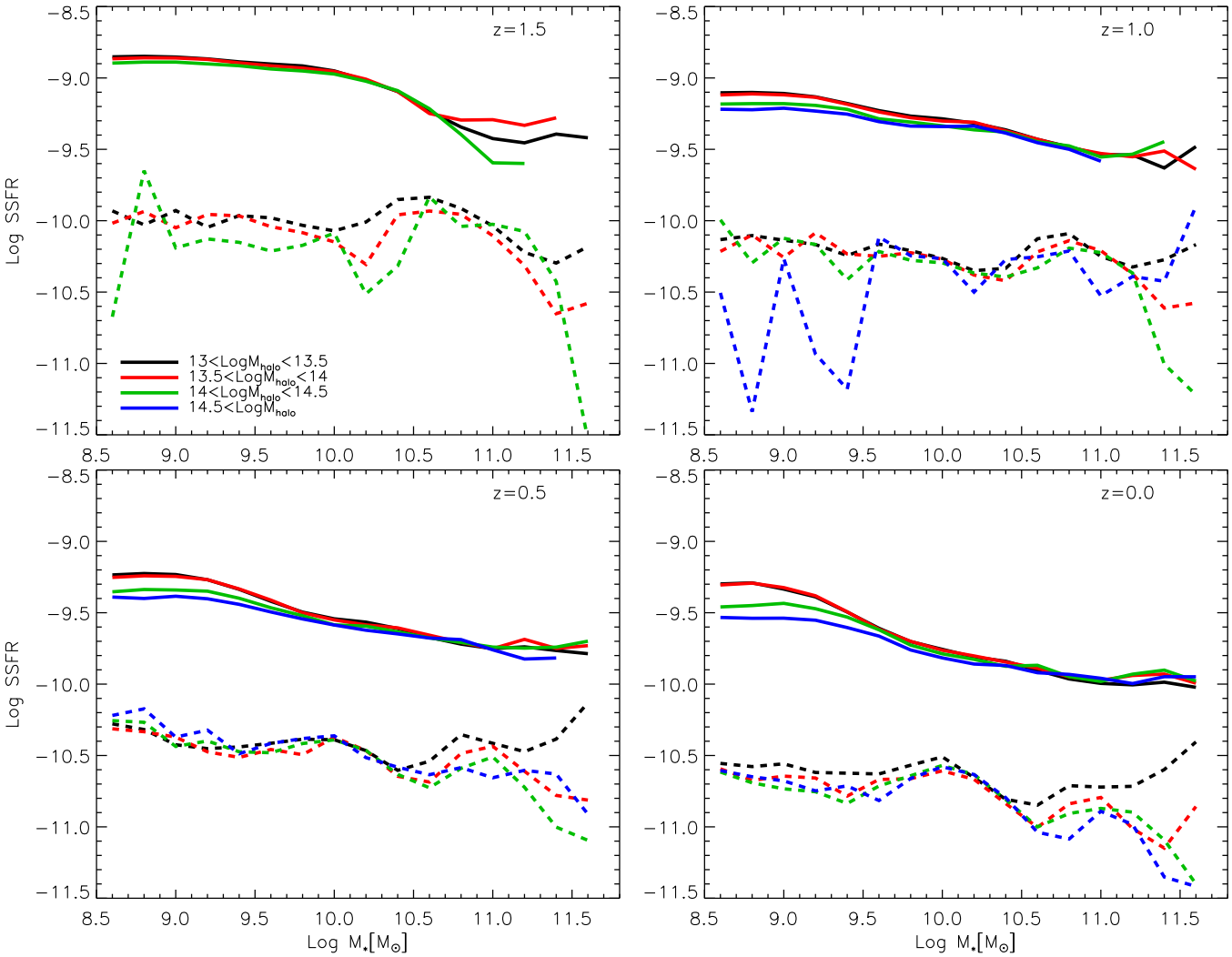

Figure 5. Evolution of the specific star formation rate–stellar mass relation as a function of redshift (different panels) for star-forming (solid lines) and quiescent (dashed lines) galaxies residing in halos of different masses, as indicated in the legend. The average 1σ scatter is around 0.15/0.2 dex for star-forming/quiescent galaxies, mostly independent of redshift and halo mass. As for the SFR shown in Figure 4, the SSFR at fixed stellar mass is independent of the environment for both star-forming and quiescent galaxies.

environment and stellar mass for galaxies in a cluster at intermediate redshift ($0.4 < z < 0.9$), found no dependence of the star formation activity on environment. Moreover, they suggest that for cluster galaxies in that redshift range, mass must be the main driver of quenching. Muzzin et al. (2012), in one of their main conclusions, state that in the redshift range they probed ($z \sim 1$), "the stellar mass is the main responsible for determining the stellar populations of both star-forming and quiescent galaxies, and not their environment." In their work, they used the clustercentric distance as a proxy of environment, and so, according to their Figure 10, where they plot the SSFR as a function of the distance from the center of the cluster (they also probed longer distances where galaxies can be classified as being in the field), quenching is not sensitive to the particular location of a given galaxy.

Their conclusion is supported by other works, such as Wetzel et al. (2012), Darvish et al. (2016), and Laganá & Ulmer (2018). Darvish et al. (2016) used a sample of star-forming and quiescent galaxies in the COSMOS field at $z < 3$, and studied the role of environment and stellar mass on galaxy properties, in particular the evolution of the SFR and SSFR with overdensity (as a proxy of the environment) as a function of redshift. For all galaxies, although at $z > 1$ the SFR and SSFR do not depend on the overdensity (i.e., no environmental dependence), at lower redshift they strongly do. However, once star-forming systems are isolated, no clear dependence on the overdensity is seen at any redshift. This is in good agreement with our results, and in general with a picture where the environment does not influence the star formation activity of star-forming galaxies, but it can increase the probability of a given galaxy becoming quiescent. Indeed, it has been pointed out by many authors (Patel et al. 2009; Peng et al. 2010; Darvish et al. 2016; Pintos-Castro et al. 2019) that the fraction of quiescent galaxies strongly depends on the environment, but the SFR and SSFR of star-forming galaxies are independent of environment (Muzzin et al. 2012; Wetzel et al. 2012; Koyama et al. 2013; Darvish et al. 2016; Laganá & Ulmer 2018; this work).

It must be noted, however, that there are also claims of an environmental dependence on the SFR for star-forming galaxies (e.g., von der Linden et al. 2010; Patel et al. 2011; Woo et al. 2013; Tran et al. 2015; Schaefer et al. 2017). As discussed previously, part of the tension can be attributed to different reasons. We have already cited the importance of the

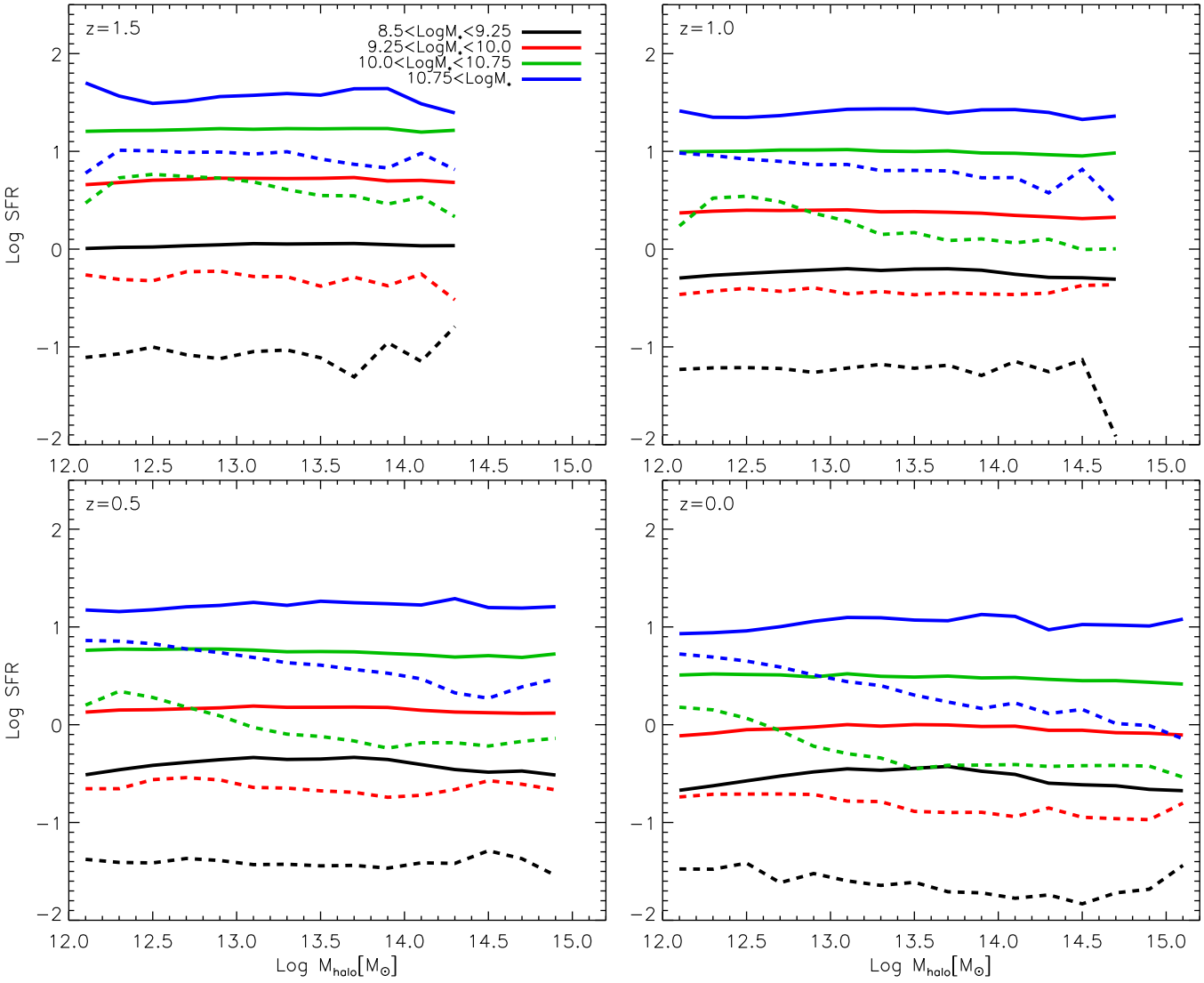

Figure 6. Evolution of the star formation rate—halo mass relation as a function of redshift (different panels) for star-forming (solid lines) and quiescent (dashed lines) galaxies in different stellar mass bins, as indicated in the legend. The average 1σ scatter is around 0.15/0.2 dex, for star-forming/quiescent galaxies, independently of redshift and stellar mass. The SFR is independent of halo mass (as found in Figure 4) at any redshift, but at a given halo mass, the SFR is strongly dependent on stellar mass, for both star-forming and quiescent galaxies. This is a clear evidence of mass quenching.

method of separating star-forming from quiescent galaxies (Section 3), but different SFR indicators, the selection of the environment, and cosmic variance might play a non-negligible role, in particular the environment itself, which is still probably one of the most undefined (or ill-defined) galaxy properties in astrophysics. Its definition ranges from halo mass in which galaxies reside to clustercentric distance (or normalized by the virial radius of the cluster) and local overdensity within the *N*th-nearest neighbor. Another possible source for the disagreement between the predictions of our model and the results of the studies quoted above might be found in the sensitivity of the model parameters, especially in the delay time and quenching timescale (τ_s) of satellites. In this regard, we ran the model by applying reasonable variations (up to $\pm 30\%$ on the delay time $t_{\rm delay}$ and $\pm 50\%$ on the random fraction f_τ), finding no appreciable difference with the results obtained in this analysis. However, higher percentages would change the evolution of the predicted SMF and worsen its comparison with the observed one, which would go against the main goal of our model.

It appears clear from our analysis that stellar mass is the main driver of galaxy quenching, at any redshift probed in this study. This is the main conclusion of our work, which fits well with the growing observational evidence that supports it, at least down to redshift $z \sim 0.5$ (e.g., Laganá & Ulmer 2018). The novelty of this paper is to extend mass quenching as the primary mode of shutting down star formation in star-forming galaxies down to the present time.

Before concluding, it is important to quote a number of observational results that imply a connection between mass and environmental quenching. These two modes of quenching were treated as separable by many authors (e.g., Peng et al. 2010; Muzzin et al. 2012, this work and many others), but there is growing consensus (mainly among observers) that environmental quenching is mass dependent in very dense environments such as the cores of galaxy clusters (Balogh et al. 2016; Darvish et al. 2016; Kawinwanichakij et al. 2017; Papovich et al. 2018; Pintos-Castro et al. 2019). All of these quoted works found a mutual dependence between the mass and environmental quenching efficiencies, from $z > 1$

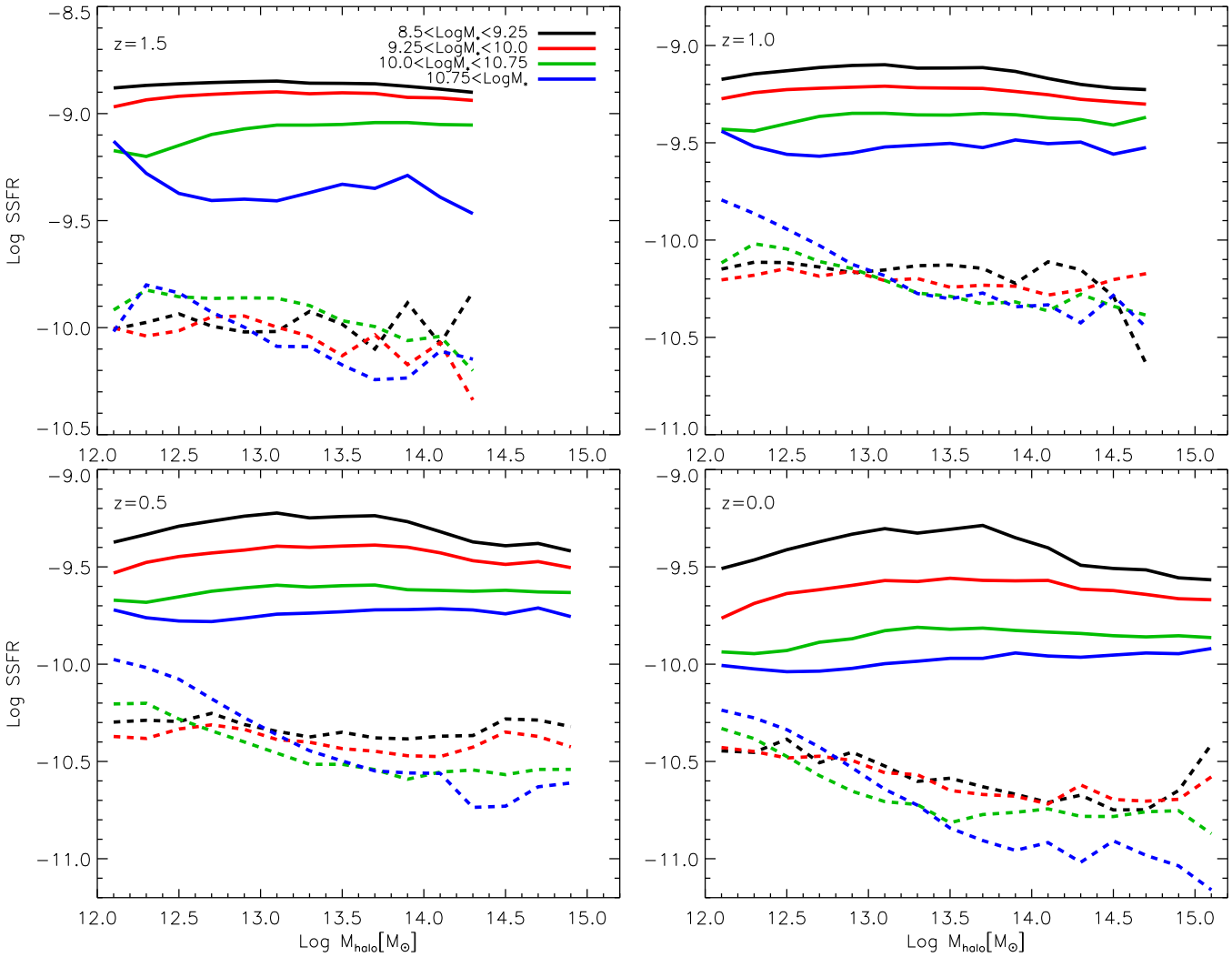

Figure 7. Evolution of the specific star formation rate—halo mass relation as a function of redshift (different panels) for star-forming (solid lines) and quiescent (dashed lines) galaxies in different stellar mass bins, as indicated in the legend. The average 1σ scatter is around 0.1/0.15 dex, for star-forming/quiescent galaxies, independently on redshift and stellar mass. Similarly to Figure 6, the same trend is found for the SSFR of the star-forming sample, while the trend does not appear clear for the quiescent one.

(Kawinwanichakij et al. 2017) to $z \sim 0.4$ (Pintos-Castro et al. 2019). The analysis done in this work does not allow us to either confirm or prove wrong such a (important) statement. In principle, if mass and environmental quenching are mutually dependent, this should be seen in Figure 8, where the SFR/SSFR of star-forming galaxies in each stellar mass bin should depend on the distance from the cluster core, and they do not. However, mass and environmental quenching efficiencies have very precise definitions. The environmental quenching efficiency is usually defined as the increase of the fraction of quiescent galaxies at a given distance from the cluster center with respect to the field, normalized by the fraction of star-forming galaxies in the field. The mass-quenching efficiency is defined in a similar way by means of a characteristic mass at which almost all galaxies at a given distance bin are star-forming. The information in Figure 8 is then not enough to make a fair comparison with the works cited above. We aim to address this point with a full analysis in a forthcoming paper.

5. Conclusions

We studied the roles of stellar mass and environment in quenching galaxies by taking advantage of an analytic model of galaxy formation. The model was set in order to match the evolution of the global stellar mass function from high to low redshifts and, at the same time, to give reasonable predictions of the SFH of galaxies. From the analysis done in this work we can conclude the following:

1. The SFR/SSFR–M_* relations are independent of the environment at any redshift probed, $0 < z < 1.5$, for both star-forming and quiescent galaxies.
2. The SFR–$M_{\rm halo}$ relation strongly depends on stellar mass at any redshift probed, for both star-forming and quiescent galaxies.
3. The SSFR–$M_{\rm halo}$ relation strongly depends on stellar mass at any redshift probed for star-forming galaxies, while the trend is not clear for the quiescent sample.
4. Overall, less massive galaxies are more star-forming, in agreement with the downsizing scenario for which less massive galaxies quench on longer timescales.

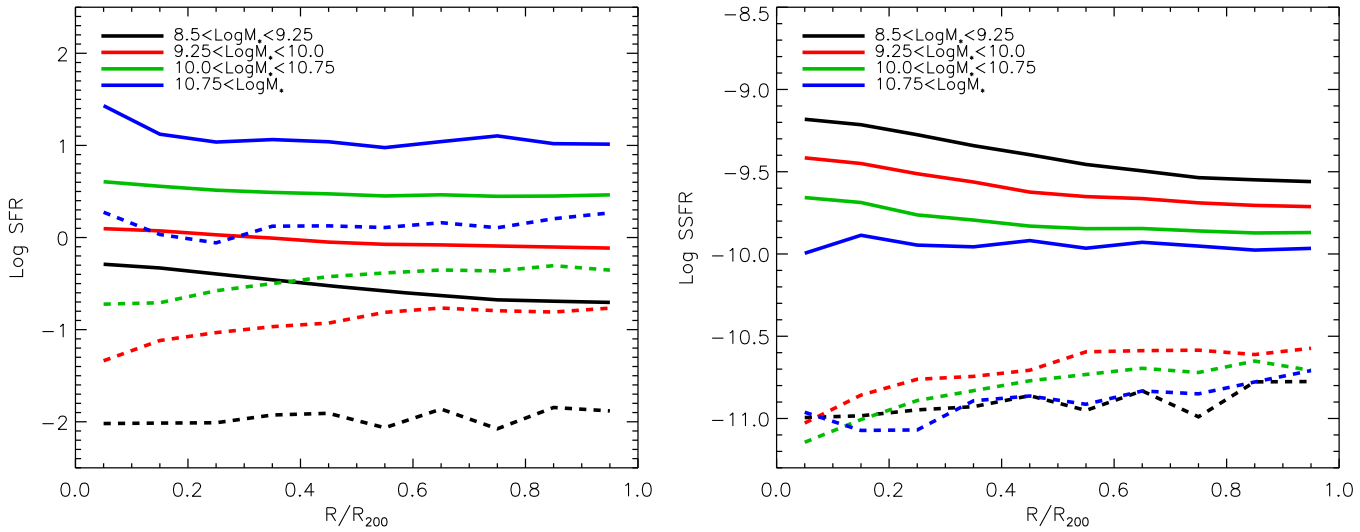

Figure 8. Star formation rate (left panel) and specific star formation rate (right panel) of star-forming (solid lines) and quiescent (dashed lines) galaxies as a function of distance from the halo center for galaxies in different stellar mass bins, at $z = 0$. The average 1σ scatter is around 0.2/0.25 dex (left panel), and 0.15/0.2 (right panel), for star-forming/quiescent galaxies, independently on stellar mass. Altogether, considering the results found above, this strongly suggests that at fixed environmental conditions, maybe those given by the typical halo mass or clustercentric distance, the SFR and SSFR depend on stellar mass.

5. The SFR and SSFR are strongly dependent on stellar mass even when the distance from the cluster core is used as a proxy for the environment (rather than the halo mass).

All these conclusions together draw a picture where stellar mass is the main driver of galaxy quenching at any redshift, not only at $z > 1$ as generally claimed in the literature. The role of environment is marginal: environmental processes must act very fast such that they do not have an effect on the star formation activity of star-forming galaxies, but can increase the probability of a galaxy becoming quiescent.

In a forthcoming paper we will address the point of the mutual dependence of the mass- and environment-quenching efficiencies by looking directly at the star-forming and quiescent fractions in galaxy clusters, and compare the predictions of our model with the newest observational evidence.

This work is supported by the National Key Research and Development Program of China (No. 2017YFA0402703), by the National Natural Science Foundation of China (Key Project No. 11733002), the Korean National Research Foundation (NRF-2017R1A2A05001116), and the NSFC grant (11825303, 11861131006). E.C. acknowledges support from the Faculty of the European Space Astronomy Centre (ESAC)—funding reference 497.

ORCID iDs

E. Contini https://orcid.org/0000-0002-2873-8598
Q. Gu https://orcid.org/0000-0002-3890-3729
J. Rhee https://orcid.org/0000-0002-0184-9589
S. K. Yi https://orcid.org/0000-0002-4556-2619

References

Abazajian, K. N., Adelman-McCarthy, J. K., Agüeros, M. A., et al. 2009, ApJS, 182, 543
Baldry, I. K., Balogh, M. L., Bower, R. G., et al. 2006, MNRAS, 373, 469
Baldry, I. K., Glazebrook, K., Brinkmann, J., et al. 2004, ApJ, 600, 681
Balogh, M., Eke, V., Miller, C., et al. 2004, MNRAS, 348, 1355
Balogh, M. L., McGee, S. L., Mok, A., et al. 2016, MNRAS, 456, 4364
Balogh, M. L., Navarro, J. F., & Morris, S. L. 2000, ApJ, 540, 113
Bamford, S. P., Nichol, R. C., Baldry, I. K., et al. 2009, MNRAS, 393, 1324
Blanton, M. R., & Berlind, A. A. 2007, ApJ, 664, 791
Blanton, M. R., Hogg, D. W., Bahcall, N. A., et al. 2003, ApJ, 594, 186
Bremer, M. N., Phillipps, S., Kelvin, L. S., et al. 2018, MNRAS, 476, 12
Brinchmann, J., Charlot, S., White, S. D. M., et al. 2004, MNRAS, 351, 1151
Cassata, P., Cimatti, A., Kurk, J., et al. 2008, A&A, 483, L39
Chabrier, G. 2003, PASP, 115, 763
Cicone, C., Maiolino, R., Sturm, E., et al. 2014, A&A, 562, A21
Contini, E., De Lucia, G., Villalobos, Á, & Borgani, S. 2014, MNRAS, 437, 3787
Contini, E., Kang, X., Romeo, A. D., & Xia, Q. 2017a, ApJ, 837, 27
Contini, E., Kang, X., Romeo, A. D., Xia, Q., & Yi, S. K. 2017b, ApJ, 849, 156
Contini, E., Yi, S. K., & Kang, X. 2018, MNRAS, 479, 932
Contini, E., Yi, S. K., & Kang, X. 2019, ApJ, 871, 24
Cooper, M. C., Gallazzi, A., Newman, J. A., & Yan, R. 2010, MNRAS, 402, 1942
Croton, D. J., Springel, V., White, S. D. M., et al. 2006, MNRAS, 365, 11
Dalla Vecchia, C., & Schaye, J. 2008, MNRAS, 387, 1431
Darvish, B., Mobasher, B., Sobral, D., et al. 2016, ApJ, 825, 113
Davies, L. J. M., Robotham, A. S. G., Lagos, C. d. P., et al. 2019, MNRAS, 483, 5444
Dekel, A., & Silk, J. 1986, ApJ, 303, 39
De Lucia, G., Hirschmann, M., & Fontanot, F. 2019, MNRAS, 482, 5041
De Propris, R., Colless, M., Peacock, J. A., et al. 2004, MNRAS, 351, 125
Dressler, A. 1980, ApJ, 236, 351
Fabian, A. C. 2012, ARA&A, 50, 455
Fang, J. J., Faber, S. M., Koo, D. C., & Dekel, A. 2013, ApJ, 776, 63
Farouki, R., & Shapiro, S. L. 1981, ApJ, 243, 32
Fillingham, S. P., Cooper, M. C., Pace, A. B., et al. 2016, MNRAS, 463, 1916
Fossati, M., Wilman, D. J., Mendel, J. T., et al. 2017, ApJ, 835, 153
Franx, M., van Dokkum, P. G., Förster Schreiber, N. M., et al. 2008, ApJ, 688, 770
Gallazzi, A., Brinchmann, J., Charlot, S., & White, S. D. M. 2008, MNRAS, 383, 1439
Gunn, J. E., & Gott, J. R., III 1972, ApJ, 176, 1
Kang, X., Li, M., Lin, W. P., & Elahi, P. J. 2012, MNRAS, 422, 804
Kauffmann, G., Heckman, T. M., White, S. D. M., et al. 2003, MNRAS, 341, 33
Kauffmann, G., White, S. D. M., Heckman, T. M., et al. 2004, MNRAS, 353, 713
Kawinwanichakij, L., Papovich, C., Quadri, R. F., et al. 2017, ApJ, 847, 134
Kimm, T., Somerville, R. S., Yi, S. K., et al. 2009, MNRAS, 394, 1131
Koyama, Y., Smail, I., Kurk, J., et al. 2013, MNRAS, 434, 423
Laganá, T. F., & Ulmer, M. P. 2018, MNRAS, 475, 523
Larson, R. B. 1974, MNRAS, 169, 229

Larson, R. B., Tinsley, B. M., & Caldwell, C. N. 1980, ApJ, 237, 692
Leja, J., van Dokkum, P. G., Franx, M., & Whitaker, K. E. 2015, ApJ, 798, 115
Maller, A. H., Berlind, A. A., Blanton, M. R., & Hogg, D. W. 2009, ApJ, 691, 394
Moore, B., Katz, N., Lake, G., Dressler, A., & Oemler, A. 1996, Natur, 379, 613
Moore, B., Lake, G., Quinn, T., & Stadel, J. 1999, MNRAS, 304, 465
Muzzin, A., Marchesini, D., Stefanon, M., et al. 2013, ApJ, 777, 18
Muzzin, A., Wilson, G., Yee, H. K. C., et al. 2012, ApJ, 746, 188
Noeske, K. G., Weiner, B. J., Faber, S. M., et al. 2007, ApJL, 660, L43
Pallero, D., Gómez, F. A., Padilla, N. D., et al. 2019, MNRAS, 488, 847
Papovich, C., Kawinwanichakij, L., Quadri, R. F., et al. 2018, ApJ, 854, 30
Pasquali, A., van den Bosch, F. C., Mo, H. J., Yang, X., & Somerville, R. 2009, MNRAS, 394, 38
Patel, S. G., Holden, B. P., Kelson, D. D., Illingworth, G. D., & Franx, M. 2009, ApJL, 705, L67
Patel, S. G., Kelson, D. D., Holden, B. P., Franx, M., & Illingworth, G. D. 2011, ApJ, 735, 53
Peng, Y.-j., Lilly, S. J., Kovač, K., et al. 2010, ApJ, 721, 193
Peng, Y.-j., Lilly, S. J., Renzini, A., & Carollo, M. 2012, ApJ, 757, 4
Pintos-Castro, I., Yee, H. K. C., Muzzin, A., Old, L., & Wilson, G. 2019, ApJ, 876, 40
Poggianti, B. M., Moretti, A., Gullieuszik, M., et al. 2017, ApJ, 844, 48
Popesso, P., Rodighiero, G., Saintonge, A., et al. 2011, A&A, 532, A145
Schaefer, A. L., Croom, S. M., Allen, J. T., et al. 2017, MNRAS, 464, 121
Sobral, D., Best, P. N., Smail, I., et al. 2011, MNRAS, 411, 675
Tomczak, A. R., Quadri, R. F., Tran, K.-V. H., et al. 2016, ApJ, 817, 118
Tran, K.-V. H., Nanayakkara, T., Yuan, T., et al. 2015, ApJ, 811, 28
Trussler, J., Maiolino, R., Maraston, C., et al. 2018, arXiv:1811.09283
Vale, A., & Ostriker, J. P. 2004, MNRAS, 353, 189
van den Bosch, F. C., Aquino, D., Yang, X., et al. 2008, MNRAS, 387, 79
van der Wel, A., Franx, M., van Dokkum, P. G., et al. 2014, ApJ, 788, 28
von der Linden, A., Wild, V., Kauffmann, G., White, S. D. M., & Weinmann, S. 2010, MNRAS, 404, 1231
Vulcani, B., Poggianti, B. M., Finn, R. A., et al. 2010, ApJL, 710, L1
Weinmann, S. M., van den Bosch, F. C., Yang, X., & Mo, H. J. 2006, MNRAS, 366, 2
Weisz, D. R., Dolphin, A. E., Skillman, E. D., et al. 2015, ApJ, 804, 136
Wetzel, A. R., Tinker, J. L., & Conroy, C. 2012, MNRAS, 424, 232
Wetzel, A. R., Tinker, J. L., Conroy, C., & van den Bosch, F. C. 2013, MNRAS, 432, 336
Woo, J., Dekel, A., Faber, S. M., et al. 2013, MNRAS, 428, 3306
Wuyts, S., Förster Schreiber, N. M., van der Wel, A., et al. 2011, ApJ, 742, 96